Investigations on the role of impaired lysosomes of macrophages in disease

Lienden, M.J.C. van der

Chapter 6

Transcriptional regulation of macrophage lysosome biogenesis in vitro and in the obese adipose tissue

Contributing authors:
M.J.C. van der Lienden[1], H.J.P. van der Zande[2], F. Otto[2], C. Oses[3], N. Claessen[4], M. Verhoek[1], J. Aten[4], J.M.F.G. Aerts[1], B. Guigas[2], M. Aouadi[3] & M. van Eijk[5]. *To be submitted.*

[1]Department of Medical Biochemistry, Leiden Institute of Chemistry, Leiden University, The Netherlands.
[2] Department of Parasitology, Leiden University Medical Centre, Leiden, The Netherlands.
[3] Department of Medicine, Integrated Cardio Metabolic Centre, Karolinska Institutet, Huddinge, Sweden.
[4] Department of Pathology, Academic Medical Centre, University of Amsterdam, Amsterdam, the Netherlands.
[5] Department of Medical Biochemistry, Leiden Institute of Chemistry, Leiden University, The Netherlands. m.c.van.eijk@LIC.leidenuniv.nl

Abstract

Recent studies suggest an important role for the lysosome in acquired metabolic disorders such as obesity. Obese adipose tissue macrophages (ATMs) scavenge lipid-rich debris and exhibit marked lysosomal storage and increased lysosomal mass. In line, GPNMB, a marker for lysosomal perturbation, is highly elevated in obese ATMs. In this study, the role of transcription factors that drive lysosomal biogenesis in macrophages was characterized. Interference with lysosomal integrity triggers a cellular response through three transcription factors that belong to the microphthalmia-transcription factor E (MiT/TFE) family. In cultured RAW264.7 cells TFEB, TFE3 and MITF all contribute to lysosomal biogenesis. Ablation of these TFs in ATMs of leptin deficient obese mice lowered adiponectin and worsened glucose metabolism. Altogether, we report a complex transcriptional regulation of the lysosome in macrophages. Our data suggest an adaptive role of lysosomal apparatus in ATMs that reduces the burden of sustained metabolic overload.

Introduction

The lysosome is an acidic, membrane enclosed organelle that is involved in the degradation of macromolecules derived from endocytosis, macropinocytosis and phagocytosis. Intracellular cargo enters the lysosome via (macro-) autophagy, a process that facilitates removal of dysfunctional organelles and misfolded protein.[1]

The identification of a transcriptional machinery that drives lysosomal biogenesis upon high catabolic demand has put the lysosome at the forefront of metabolic regulation. Predominant in this cellular response is considered to be the microphthalmia-transcription factor E (MiT/TFE) subfamily of basic helix-loop-helix (bHLH) transcription factors (TFs).[2] This subfamily of leucine zipper regulatory proteins consists of transcription factor EB (TFEB), transcription factor E3 (TFE3), melanogenesis associated transcription factor (MITF) and transcription factor EC (TFEC).[3] The MiT/TFE subfamily was associated with lysosomal biogenesis upon identification of TFEB as primary binding protein to a common sequence upstream of lysosomal genes, the so called Coordinated Lysosomal Expression and Regulation (CLEAR) element.[4] These factors homo- or heterodimerize to bind DNA sequences involved in cellular metabolism.[5] TFEB and TFE3 are ubiquitously expressed, whereas MITF is largely restricted to pigmented cells such as melanocytes and retinal epithelium cells, as well as to myeloid cells of the immune system, osteoclasts, and stem cells of the hair follicle.[3,6].

TFEB, TFE3 and MITF are subjected to phosphorylation by Mammalian target of rapamycin complex 1 (mTORC1), an established master regulator of cell growth that resides at the cytosolic side of the lysosomal membrane.[7–10] At this position, mTORC1 functions as a key signaling hub for nutrients and hormonal pathways.[11] Under basal, nutrient rich conditions, RAG GTPases facilitate lysosomal localization of mTORC1 that allows proximity with its activator protein Ras homologue enriched in brain (RHEB). Likewise, RAG GTPases and 14-3-3 proteins associate with phosphorylated MITF, TEB and TFE3 and sequester them in the cytosol.[12–15] With respect to TFEB, a serine residue is phosphorylated by active mTORC1.[13,16] A homologous serine residue can be found on MITF and its phosphorylation was previously shown to be important for cytosolic retention by 14-3-3 proteins.[17] Inhibition of mTORC1 results in dephosphorylation of TFEB and its nuclear localization. This was initially achieved artificially through selective inhibition of mTORC1 by a commonly used drug Torin 1, as well as through lysosomal amino acid starvation.[4,13,18,19] Treatment with conventional lysosomal stressors such as the undegradable sugar sucrose or elevation of lysosomal pH by the lysosomotropic compound chloroquine, induced a similar nuclear translocation of TFEB, MITF and TFE3. Moreover, evidence suggests that TFEB and other TFs exhibit enhanced transcriptional activity in diseases that are characterized by a lysosomal defect.[4,15,20–22].

Perturbed lysosomal function is also implicated in other biological processes such as longevity, and in pathologies like cancer and neurodegeneration.[23–26] Among the most common acquired metabolic disorders in which lysosomal function has been suggested to play an important role is obesity and its associated pathologies classified as the metabolic syndrome.[27,28] Xu et al. discovered a lysosome driven program of lipid degradation in adipose tissue macrophages (ATMs) upon obesity and ultrastructural analysis revealed a foamy appearance of obese ATMs.[29] In line with this, glycoprotein non metastatic protein B (GPNMB), a marker for lysosomal problems in macrophages, is dramatically increased

in obese mice and, to a lesser extent, in men.[30,31] It was furthermore shown in RAW264.7 cells that GPNMB expression was induced upon palmitate feeding (not oleate) and upon exposure to the lysosomotropic agent chloroquine, an induction that was driven by MITF. Moreover, GPNMB was shown to potentiate arginase-1 production upon IL-4 stimulation, thereby associating GPNMB with an immunomodulatory phenotype.[30] The immunological status of the adipose tissue is largely influenced by the bidirectional communication between adipocytes and macrophages. Macrophages react to adipocyte derived factors hormones such as adiponectin, which sensitizes tissues for insulin and alleviate toxic lipid accumulation (lipotoxicity) and inflammation.[32] This balance is disturbed upon obesity.

Despite the increased understanding of the machinery that orchestrates lysosomal adaptation, it remains largely unclear to what extent adaptive lysosomal biogenesis contributes to pathology. Here, we test the contribution of MITF, TFEB and TFE3 in regulating increased lysosomal demand. Significance of these TFs in obese ATMs was characterized through recently developed ATM specific siRNA delivery molecules called glucan encapsulated particles (Gerps).[33,34] A combinatorial approach was employed, targeting the TFs in ATMs simultaneously to highlight the importance of lysosomal adaptation within ATMs.

Results

In vitro analysis of MiT/TFE knockdown in cultured RAW264.7 cells

TFs belonging to the MiT/TFE subfamily are established regulators of lysosomal gene transcription, but redundancy and mutual exclusivity are incompletely understood. Macrophages express Tfeb, Tfe3 as well as Mitf. To impair lysosomal regulation macrophage-like cells, an siRNA-based approach was applied to specifically knock-down either MITF, TFEB or TFE3 in cultured RAW264.7 cells. Transfection with siRNA targeting *Mitf* in RAW264.7 cells resulted in knock down of *Mitf*, along with an increase in expression of *Tfeb* and *Tfe3* (**Figure 1A**). In contrast, successful knock down of *Tfeb* did not alter expression of *Mitf* and *Tfe3*. Knock-down of *Tfe3* resulted in a concomitant increase in *Mitf*, but not *Tfeb*. At the level of protein, knock-down could be verified by western blot (**Figure 1B**). The use of different oligonucleotide sequences for one of the respective targets confirmed a specific effect of the siRNA oligonucleotides used (**Supplemental figure 1A**). Immunohistochemistry provided additional proof for reduced protein abundance of respective target genes (**Figure 1C**). Of note, knock down of either MITF, TFEB or TFE3 with or without sucrose supplementation did not markedly affect nuclear translocation of the other TFs, suggesting that reduced presence of one MiT/TFE-member did not lead to changes in localization of subfamily members (**Supplemental figure 1B**). Subtle changes in MiT/TFE nuclear localization upon knock down of homologous TFs however, cannot be ruled out.

In the presence of the mild lysosomal stressor HEPES, a similar pattern with respect to *Mitf, Tfeb* and *Tfe3* RNA expression was observed upon each respective knock down (**Figure 1D**). Expression of lysosomal genes *Gpnmb*, *CtsD*, *Lamp1* and *Atp6v1a* and inflammatory genes *Ccl2* and *Tnfa* were elevated upon HEPES supplementation (**Supplemental figure 2A**) and were unaltered or further increased upon knock down of either *Mitf, Tfeb* or *Tfe3* (**Figure 1D**). This unanticipated increase could be explained by

cross regulation. It was therefore decided to use a combinatorial knockdown approach, in which two or three transcription factors are knocked down simultaneously. In DMEM cultured (basal conditions) RAW264.7 cells, *Tfeb* showed a more than two-fold induction upon simultaneous knock-down of *Mitf* and *Tfe3*, whereas *Mitf* exhibited increased expression upon combined knock-down of Tfeb and Tfe3 (**Figure 1E**). *Tfe3* did not seem to be subjected to a regulatory feedback in the experimental set up. The changes in expression levels of *Mitf, Tfeb* and *Tfe3* remained the same in the presence of HEPES (**Figure 1F**). Next, we analysed the impact of the various knockdown combinations on lysosomal genes in the presence of HEPES. A combination of either reduced *Mitf* or *Tfe3* with reduced *Tfeb* showed reduction in the expression of *Gpnmb* in HEPES stimulated cells (**Figure 1F**). Surprisingly, knock-down of all three transcription factors was necessary to induce a significant reduction in *CtsD* and *Atp6v1a*. Of note, lysosomal and inflammatory genes were altered only to a limited extend under basal conditions (**Supplemental figure 2B**)

Analysis of inflammatory gene expression revealed that simultaneous knock-down of *Tfeb* and *Tfe3* induced an increase in *Ccl2* expression, but not *Tnfa* expression (**Supplemental figure 2C**). Additional knock-down of *Mitf* abolished this increase. In conclusion, simultaneous knock-down of *Mitf, Tfeb* and *Tfe3* resulted in the most potent reduction in target gene expression as measured by *Gpnmb, Cathepsin D* and *Lamp1*, without triggering upregulation of *Ccl2*.

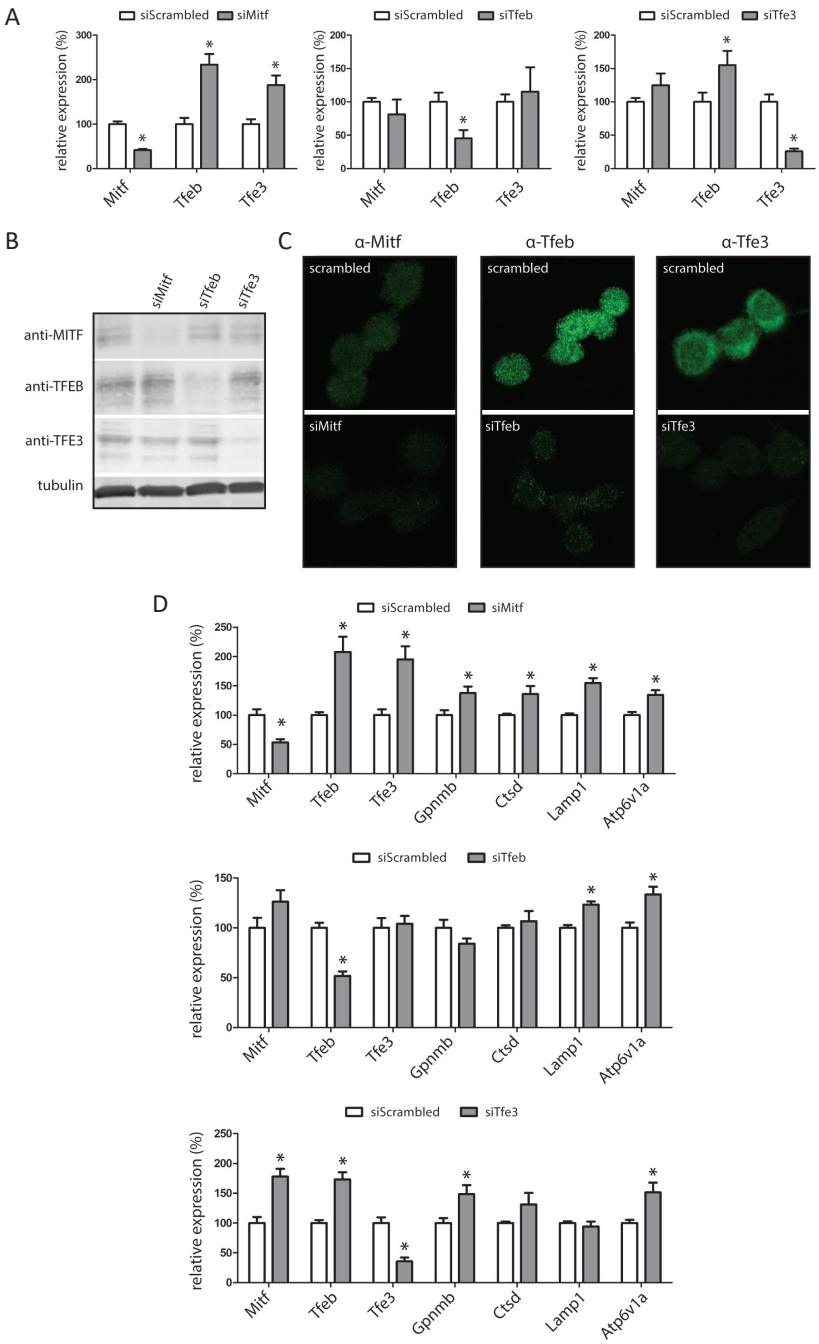

Figure 1. In vitro analysis of MiT/TFE knockdown in cultured RAW264.7 cells; (***A***) *Real-time (Rt) qPCR RNA analysis on Mitf, Tfeb and Tfe3 gene expression in RAW264.7 macrophages subjected to siRNA mediated knock down under basal conditions;* (***B***) *Western blot analysis of siRNA treated RAW264.7 macrophages;* (***C***) *Immunohistochemical analysis of siRNA mediated knock down of Mitf, Tfeb and Tfe3 in RAW264.7 cells cultured in DMEM and in DMEM supplemented with 80mM Sucrose;* (***D***) *Rt qPCR expression analysis on Mi/TEF and lysosomal gene expression of HEPES*

treated RAW264.7 cells upon single MiT/TFE knock-down; ***Below*** *-> (****E****) Rt qPCR on target genes of Mitf, Tfeb and Tfe3 through combined knock down of Mitf/Tfeb, Mitf/Tfe3, Tfeb/Tfe3 or Mitf/Tfeb/Tfe3 resp under basal conditions; (****F****) MiT/TFE and lysosomal gene expression of HEPES treated RAW264.7 cells upon combinatorial MiT/TFE knock-down.*

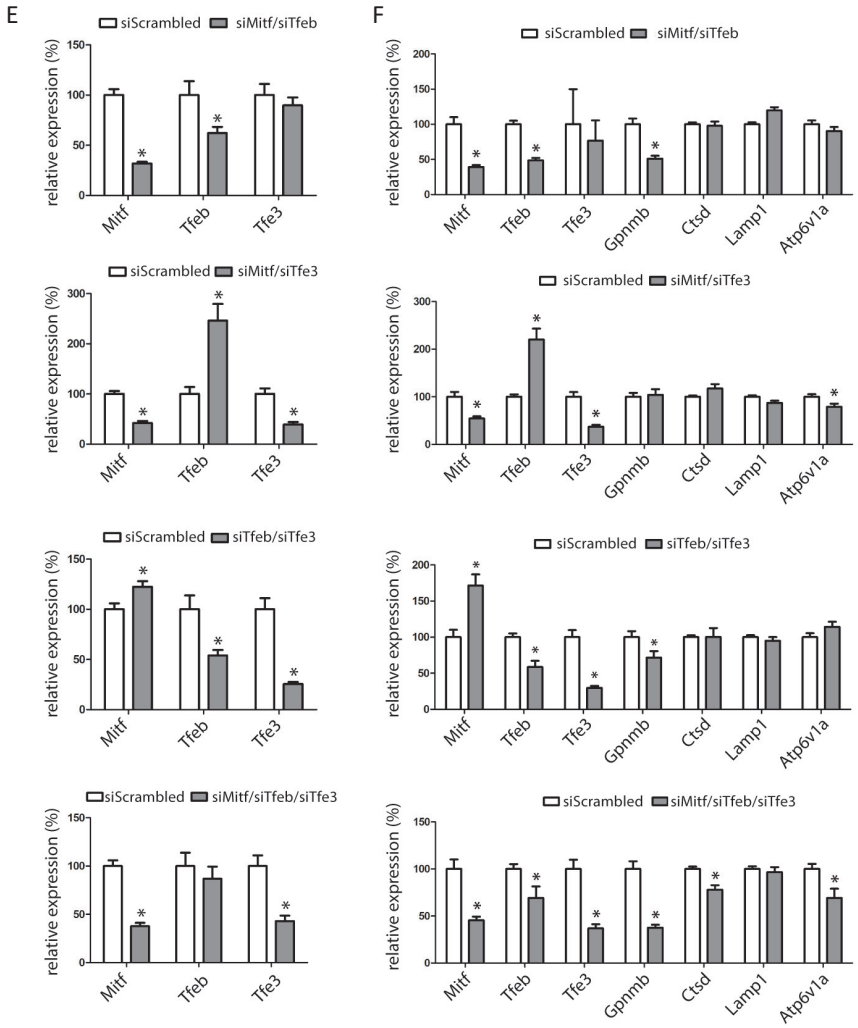

Validation Gerp particles in RAW264.7 cells

To investigate the impact of MITF, TFEB and TFE3 *in vivo,* we optimized a macrophage specific siRNA delivery method through yeast derived glucan shells called glucan encapsulated particles (Gerps). Through this method we aimed to simultaneously knock down *Mitf*, *Tfeb* and *Tfe3*. Firstly, functionalized yeast derived glucan shells were prepared to deliver siRNA in RAW264.7 cells according to the described protocol.[33,34] In cultured RAW264.7 cells, addition of Gerp-siRNA complexes resulted in internalization and accumulation of these Gerps inside the macrophage (**Figure 2A**). RNA expression analysis revealed knock-down of all three TFs (**Figure 2B**).

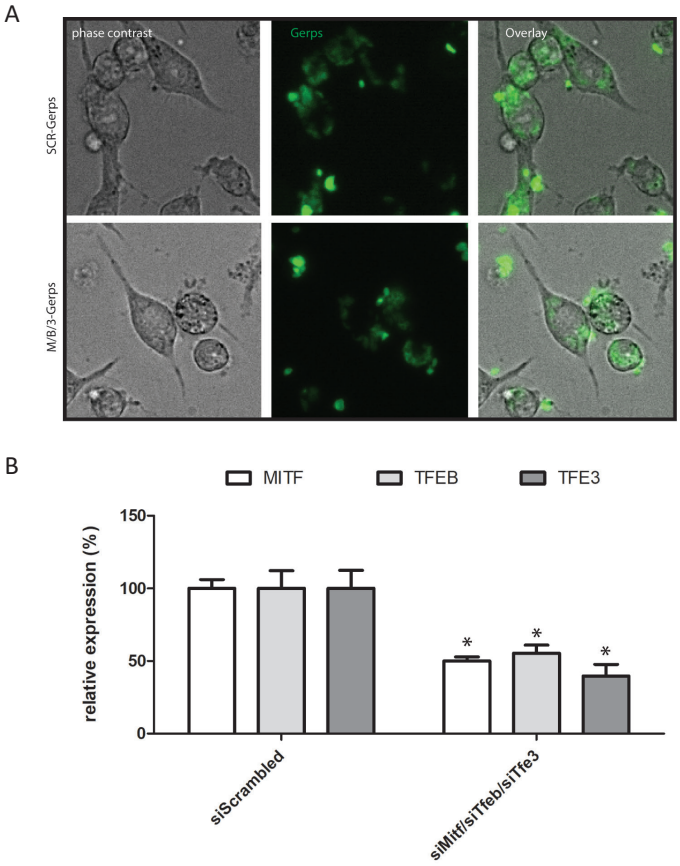

***Figure 2. Validation of Gerp-siRNA complex treatment in RAW264.7 cells**; (**A**) Fluorescence microscopy of RAW264.7 cells treated with FITC-labelled Gerp-siRNA particles; (**B**) Rt qPCR analysis of MiT/TFE genes in RAW264.7 macrophages subjected to Gerp-siRNA treatment.*

Lowering of adiponectin expression in total EWAT upon treatment of obese mice with MiT/TFE siRNA Gerp particles

Since accumulating evidence suggests that obese ATMs exhibit increased lysosomal content, this methodology was employed to study the contribution of lysosomal biogenesis in ATMs to the integrity of adipose tissue and progression of obesity in leptin deficient mice (Ob/Ob). FITC-labelled Gerps were loaded with either scrambled siRNA or siRNA targeting *Mitf*, *Tfeb* and *Tfe3* simultaneously. The siRNA-Gerp complexes were injected daily into the peritoneal cavity of 9 weeks old leptin deficient mice for a period of 14 days. Fluorescence microscopy showed localization of Gerps inside CLSs (**Figure 3A**). Gene expression analysis on whole EWAT revealed that *Tfeb* and *Tfe3* tended to be reduced, whereas *Mitf* expression remained unchanged (**Figure 3B**). Although no differential RNA expression of *Gpnmb*, *Ctsd* and *Atp6v1a* could be detected, expression of the structural lysosomal protein *Lamp1* was significantly reduced (**Figure 3C**). Moreover, no difference in inflammatory status of epididymal fat was observed due to treatment, as measured by expression levels of cytokines *Ccl2*, *Tnfa* and macrophage markers *Emr1*(F4/80) and *Itgax* (CD11c) (**Figure 3D**).

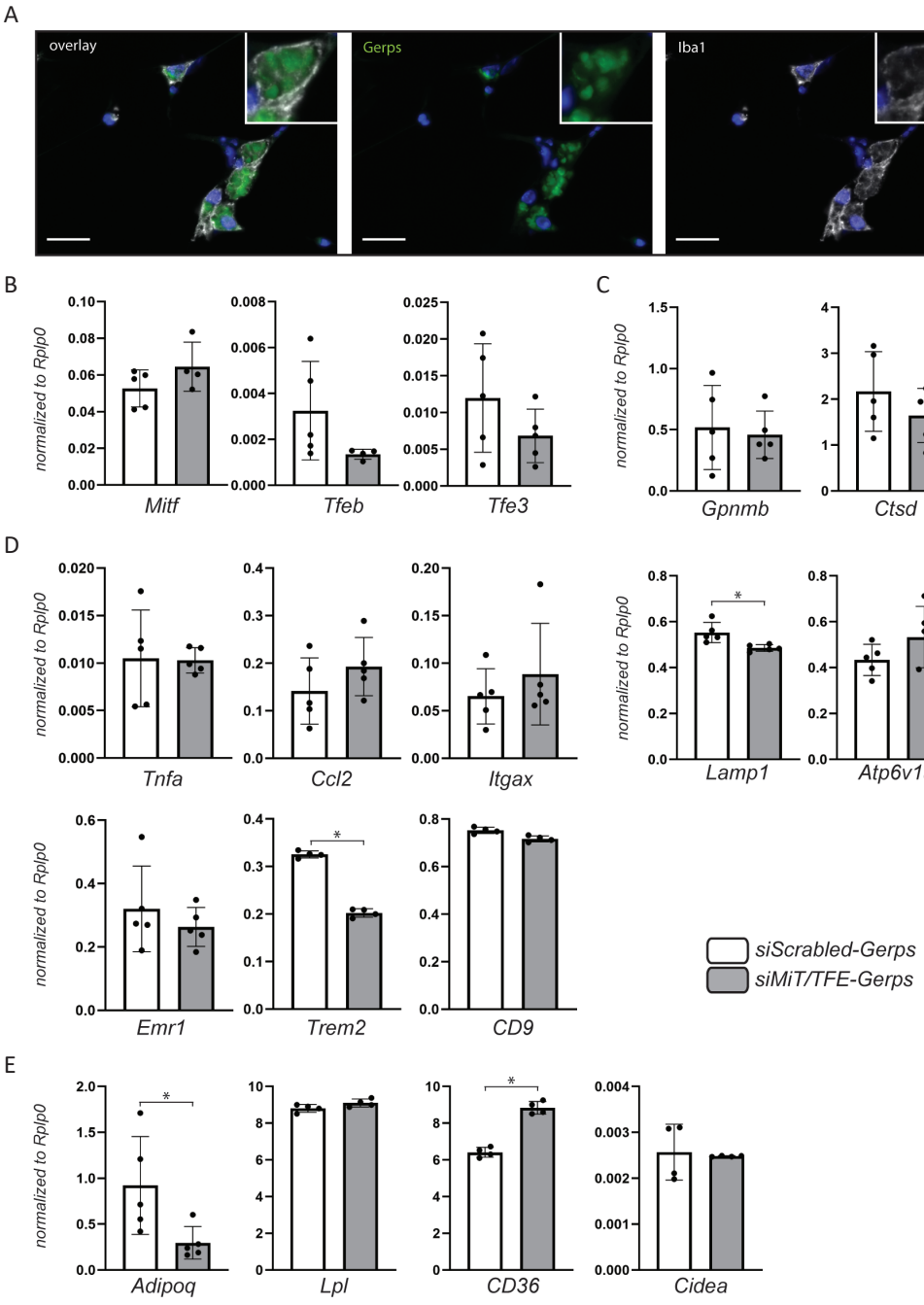

***Figure 3. Characterization of EWAT from Gerp-siRNA treated obese mice**; **(A)** Fluorescence microscopy analysis on localization of Gerps in epididymal fat of obese mice treated with siRNA-Gerp complexes, inlets show magnified cluster of ATMs, scale bar: 20μm; Rt qPCR analysis of epididymal fat on **(B)** MiT/TFE genes, **(C)** lysosomal genes, **(D)** inflammatory genes and **(E)** adiposity associated genes*

Recent studies on obesity in mice have identified a unique expression profile of ATM residing in CLSs that fundamentally differs from the classically activated macrophages.[35,36] These ATMs are characterized by *CD9*, *CD36* and *TREM2* expression and are found to be specialized in lipid uptake and degradation.[36] Upon treatment with MiT/TFE targeting siRNA, *Trem2* expression was reduced in EWAT, but not *CD9* (**Figure 3D**). Characterization of lipid related signalling and scavenging in EWAT revealed a striking reduction in expression of the insulin sensitizing adipokine *Adipoq* (Adiponectin) and an increase in the lipid scavenging receptor *CD36*. Genes encoding the lipoprotein interacting protein lipoprotein lipase (*Lpl*) and the adipocyte specific lipid droplet marker cell death-inducing DNA fragmentation factor alpha-like effector A (*Cidea*) are aberrantly expressed upon obesity, but not altered in total EWAT upon Gerp-siRNA treatment.

Since ATM specific targeting was anticipated, CD11b-enriched fractions were analysed with respect to the specificity of the Gerp-siRNA treatment, as well as the macrophage specific changes. Fluorescence microscopy could readily detect enrichment of FITC-labelled Gerps in the CD11b-positive fraction (**Figure 4A**). Unexpectedly however, knock-down of *Mitf*, *Tfeb* and *Tfe3* was not observed in $CD11b^{+}$-macrophage fraction (**Figure 4B**), while a trend towards lower expression of *Lamp1* was observed (**Figure 4C**). Other lysosomal genes did not show to be altered (**Figure 4C**). Pro-inflammatory markers *Ccl2*, *Tnfa* were not altered in the $CD11b^{+}$-fraction (**Figure 4D**). Since the ATM population exhibits high plasticity, we speculated that targeted macrophages acquired a different metabolic state and phenotype. The markers of lipid-associated macrophages *Trem2* and *CD36* were not altered (**Figure 4D** and **E**). However, *CD9*, an additional marker that identifies macrophages involved in lipid uptake and degradation, was found to be significantly reduced (**Figure 4D**). In line with a potentially altered lipid uptake, CD11b specific *Lpl* expression was similarly reduced upon Gerp treatment targeting *Mitf*, *Tfeb* and *Tfe3* (**Figure 4E**).

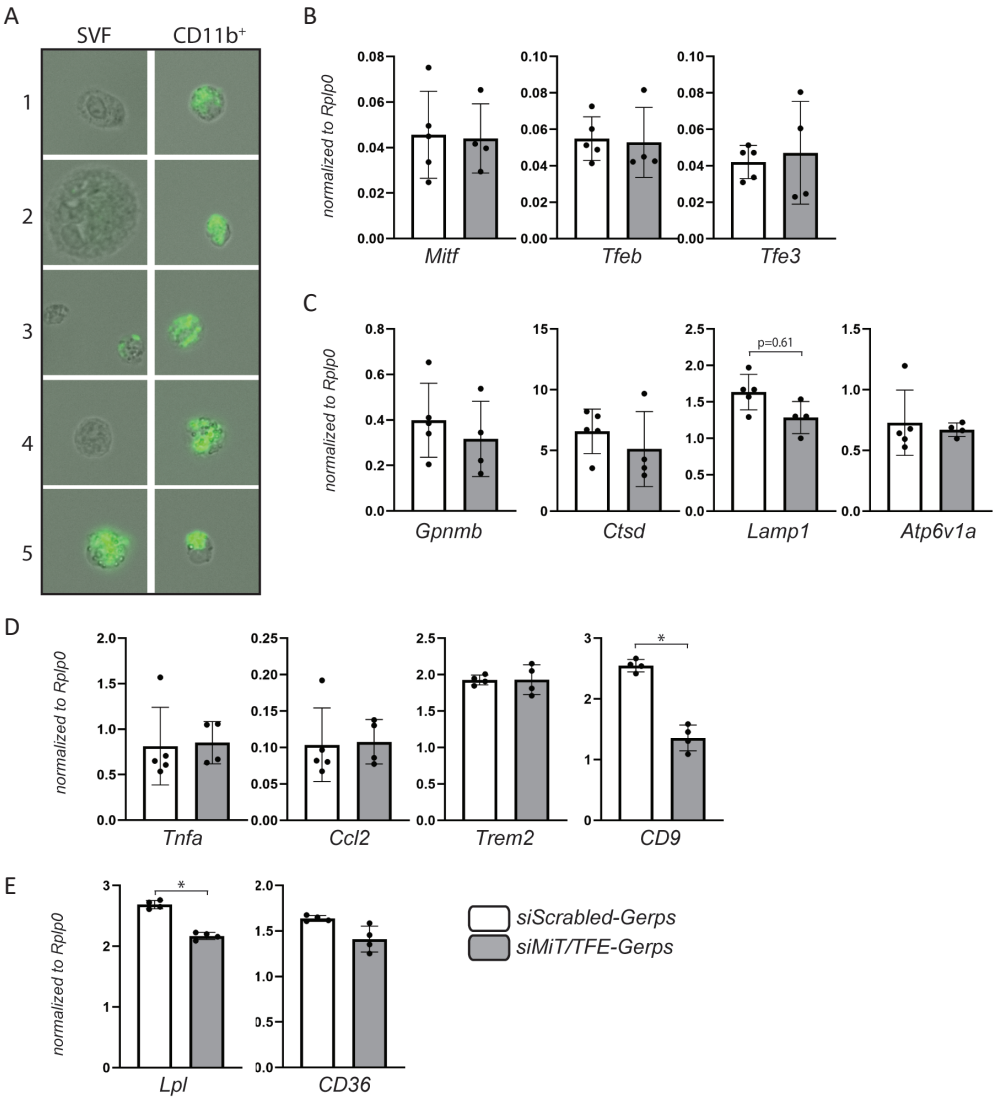

Figure 4. Characterization of EWAT obtained CD11b+-fraction from Gerp-siRNA treated obese mice*; (**A**) Fluorescence microscopy analysis of CD11b+ fraction of Gerp-siRNA treated obese epididymal fat; Rt qPCR analysis of CD11b+ fraction of Gerp-siRNA treated obese epididymal fat on (**B**) MiT/TFE genes, (**C**) lysosomal genes, (**D**) inflammatory genes and (**E**) adiposity associated genes.*

Treatment of obese mice by Gerp-MiT/TFE siRNA results in worsening of glucose tolerance

RNA expression profiles suggest that ATM specific targeting of MiT/TFE members lowers lipid associated markers of macrophages. Furthermore, the expression of the adipokine adiponectin is reduced in EWAT, which possibly impacts on systemic insulin sensitivity. To further study the impact of the siMiT/TFE-Gerp treatment on progression of obesity, metabolic parameters of treated, obese mice were analysed. At start of the treatment, metabolic parameters between groups was not different (**Supplemental figure 3**).

Strikingly, glucose tolerance significantly reduced in groups treated with siRNA oligo's targeting MiT/TFE subfamily compared to scrambled siRNA after 14 days of siRNA-Gerp treatment (**Figure 5A** and **B**). Other metabolic parameters such as average weight, fat mass percentage were not altered (**Figure 5C** and **D**). Moreover, no difference was observed in fasting insulin levels and HbA1c (**Figure 5 E** and **F**).

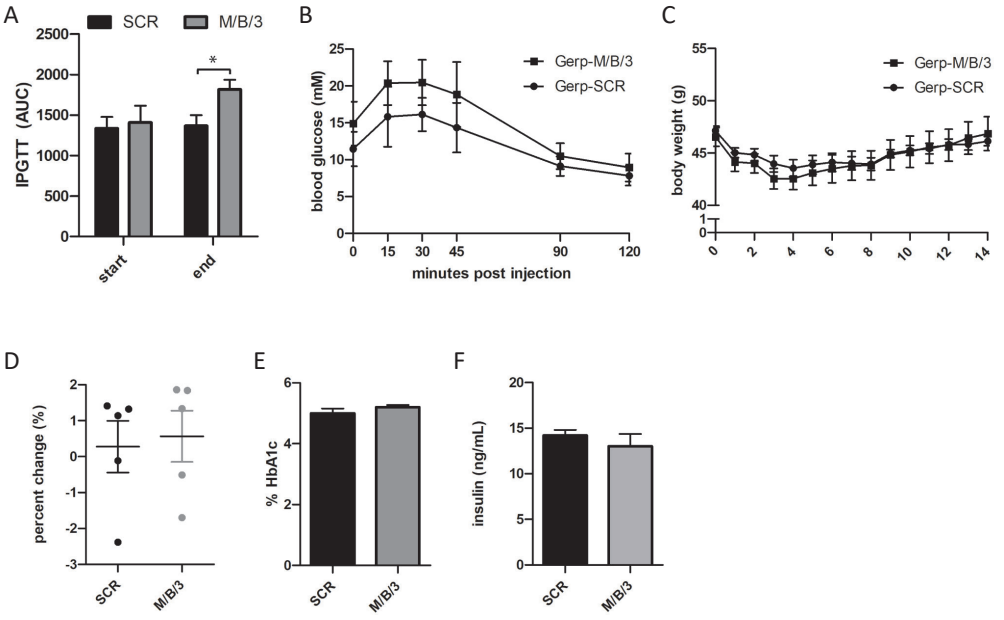

***Figure 5. Metabolic characterization of Gerp-siRNA treated obese mice**; (**A**) Area under the curves (AUC) of glucose tolerance of two weeks after treatment and (**B**) their respective curves; (**C**) Average body weight of scrambled treated group and triple knock-down group over 14 days of treatment; (**D**) Percent change in fat mass at 14 days of treatment compared to start; (**E**) Percentage change in Hb1Ac levels compared to start of the experiment; (**F**) Insulin levels at t=0 and t=14 of scrambled and triple siRNA treated groups.*

Discussion

A major factor that currently drives the interest in the lysosome is its ubiquitous role in nutrient sensing and coordination of cellular metabolism.[4,11] It has nevertheless remained enigmatic which of the known drivers of lysosomal biogenesis are redundant or crucial for their function. We previously reported transcriptional control by MITF, TFEB and TFE3 on the expression of several lysosomal genes (Chapter 2). Here, the regulatory profile of these TFs was extended by characterizing the individual and combinatorial effect of MITF, TEFB and TFE3 on expression of target genes. These data establish a compensatory feedback among MITF, TEFB and TFE3 that is dependent on the expression level of other members. Upon knock down of *Mitf* and *Tfe3* respectively, increased expression of untargeted MiT/TFE members was observed. In the case of *Mitf* targeted knock down, *Tfeb* and *Tfe3* were upregulated. In addition, regulation of target genes exhibited differential dependence on MiT/TFE members. Knock-down of *Mitf*, *Tfeb* and *Tfe3* did

not completely abolish lysosomal gene expression, which could be explained by the fact that no full knock-down was achieved. This could have allowed for residual transcriptional activity of knocked-down proteins.

Moreover, homologous MiT/TFE subfamily member TFEC is predominantly expressed in macrophages and may provide additional clues on the redundancy and exclusivity of MiT/TFE members in driving inflammatory and lysosomal gene expression. In addition to the homodimerization that occurs upon activation, heterodimerization among the MiT/TF factors has been described.[3,5] The cell specific presence of each TF, as well as the posttranscriptional (splicing) and posttranslational (phosphorylation, acetylation) processing, may determine self-regulation and promotor affinity of each subtype.[13,37,38] Quantitative assessment of dimerization affinity and DNA-binding properties may shed light onto their cell-specific action.

Alternatively, presence of other transcription factors could have contributed to lysosomal biogenesis in the absence of MiT/TE members, such as MYC, Signal transducer and activator of transcription 3 (Stat3) or zinc finger with KRAB and SCAN domains 3 (Zkscan3).[39–42]

Intriguingly, combined knock down of *Tfeb* and *Tfe3* increased pro-inflammatory *Ccl2* gene transcription under basal and HEPES stimulated conditions. When *Mitf* was simultaneously knocked down, no increase *Ccl2* expression was observed. The significance of these findings remains unclear. Earlier observations by Pastore et al. revealed that upon LPS stimulation CCL2 secretion was compromised in a *Tfeb*/*Tfe3* double knock-out RAW264.7 model compared to the wild type cell line.[43]

MiT/TFE regulation has been considered a main driver of lysosomal biogenesis, but the implication of this mechanism in tissue resident storage cells has remained incompletely understood. Moreover, a distinction between the role of these factors in ubiquitous lysosomal maintenance and compensatory (pathological) stimuli is not clear. Metabolically activated macrophages have emerged as storage cells that exhibit a unique gene expression profile along with increased lysosomal content.[29,30,44–47] These cells have been shown to fundamentally differ from the classically activated M1-macrophages that are assumed responsible for a chronic, low grade inflammatory state in obese individuals. Emerging data furthermore suggest that ATMs can serve a protective role within tissue by scavenging lipids and modulate inflammation.[30,48] The Gerp-siRNA methodology provides a unique tool to study the impact of obese ATMs on whole body metabolism through transient interference with ATM gene expression.[33,34] This way, compensatory lysosomal biogenesis in ATMs can be counteracted by interference in transcriptional regulation of lysosome genes. By fluorescence microscopy, localization of Gerps in Iba^{+}-cells in EWAT was confirmed. Moreover, Gerp-positive cells were highly enriched in the $CD11b^{+}$-fraction, which suggests that the delivery method was suitable for specific ATM targeting. A trend towards lower expression of target genes *Tfeb* and *Tfe3* was observed in the whole EWAT of MiT/TFE-Gerp treated mice, whereas no effect was observed in the $CD11b^{+}$-fraction. Although effectivity and specificity of the technique was extensively validated *in vitro*, we cannot rule out additional technicalities such as limited reach of the entire ATM population in the epididymal fat. Recent data shows that during the progression towards obesity, murine adipose tissue acquired a *Trem2* positive, lipid associated subpopulation of macrophages as characterized by single-cell sequencing.[36]

Obese *Trem2* knock-out mice manifest with dramatically increased adipocyte size and worsening of whole-body metabolism compared to obese wild type mice. Upon 14-days administration of MiT/TFE-Gerps, *Trem2* was found to be significantly lower in whole EWAT. Surprisingly, this effect was lost in the CD11b enriched fraction.[36,45,46] In contrast, *CD9*, a marker strongly associated with *Trem2*$^{+}$ LAM signature, was significantly reduced in the CD11b^{+}-fraction, whereas reduction in *CD9* expression in whole AT was not significant. The presence of distinct macrophage subpopulations could provide an explanation to the discrepancies between EWAT and CD11b^{+}-fractions. It is conceivable, for example, that the employed CD11b^{+}-enrichment protocol may not have been sensitive enough to all ATM-populations, favouring extraction of Trem2^{-} CD11b^{+}-macrophages due to either physical properties or protein expression. Since CD9 is less exclusively associated with LAMs, a treatment-effect could still be observed in the enriched fraction, while variable expression in whole EWAT could dilute this effect. Alternatively, a differential uptake of Gerp-particles by different ATM-populations or suboptimal siRNA targeting of genes could explain a large variation in certain markers. The lack of treatment-effect on Gpnmb expression in EWAT and CD11b^{+}-fraction is unexpected, since it proved the most sensitive to MiT/TFE regulation during *in vitro* validation. Again, the Gerp-siRNA particles may have reached only a subset of macrophages, diluting the effect of treatment. Expression of the ubiquitous lysosomal membrane protein *Lamp1* was however reduced in both EWAT and the CD11b^{+}-fraction of Mi/TFE-Gerp treated mice. Taken together, the expression analysis revealed a significant reduction in several genes involved in lysosome function and lipid handling in EWAT, in the CD11b^{+}-fraction or in both, concomitantly with impaired glucose clearance.

Aouadi et al. previously showed that Gerp-siRNA mediated knock-down of ATM derived lipoprotein lipase (LPL), the enzyme involved in de-esterification of lipoprotein derived lipids for cellular uptake, resulted in worsening of insulin sensitivity and a reduction in foam cell appearance, without exacerbation of the immune response.[34] Similarly, our data reveal an impaired insulin sensitivity upon interference in regulation of lysosome genes without apparent change in expression of canonical, pro-inflammatory markers *Ccl2* and *Tnfa*. The significant reduction in RNA encoding adiponectin in EWAT upon MiT/TFE knock down, an adipokine important in regulating systemic glucose metabolism, may therefore indicate that adipose tissue signalling, rather than inflammation underlies worsening of glucose sensitivity.[49] Adiponectin is exclusively produced by adipocytes and acts on many organs as potent insulin sensitizer and reducer of lipotoxicity.[32] The link between lipid-associated macrophages and the adipose tissue however remains incompletely understood.

The current study suggests that reduced MiT/TE driven lysosomal biogenesis in obese ATMs causes a concomitant reduction in expression of lipid scavenging proteins, perturbed adipose tissue signalling and worsening of systemic glucose sensitivity, independent of inflammatory status. It would be of therapeutic value to study mechanisms through which lysosome and lipid scavenging capacity of ATMs can be improved.

Material and Methods

Animals

Leptin-deficient obese mice (C57BL/6J background) were obtained from Charles River (Italy). National and local ethical committee approval was obtained for conducting animal experiments and laboratory animal welfare rules were followed (AVD nr AVD106002018660 7). Mice were kept on a chow diet for the duration of experiments. Body weight and food intake were measured weekly prior to start and daily from start of experiments on. Lean and fat mass were scanned at day 0, day 7 and day 14 by EchoMRI-100 analyzer (Echo MRI).

Prepatation of Gerps

Gerp-siRNA complexes were prepared as previously described.[50] siRNA was functionalized by a 15 minutes incubation of 3 nmol siRNA (Dharmacon) with 50 nmoles Endo-Porter (Gene Tools) at room temperature, buffered in a total volume of 20 µl by 30 mM sodium acetate pH 4.8. The functionalized siRNA solution was loaded into the glucan shells by resuspending 1 mg of FITC labelled glucan shells in the siRNA/endoporter solution, vortexed and incubated for 1 h. The siRNA-Gerp complexes were brought to a final concentration by PBS, homogenized by sonication and stored at -20°C.

Gerp-siRNA treatment of obese mice

9-weeks old mice were assigned to a treatment and control group (5 mice per group) based on fasting body weight and glucose levels. Daily, mice received intraperitoneal (i.p) treatment with one dose Gerp-siRNA up to fourteen days. One dose of prepared Gerps contained 0.2 mg of glucan shell, 10 nmol of Endo-Porter (Gene Tools) and 1 nmol of siRNA (Qiagen) in PBS (200µl). Organs were collected for assessment of specificity of the treatment and for metabolic and immunological profiling.

Monitoring metabolic parameters

Performance of the intraperitoneal glucose tolerance test (IPGTT) was performed by injection of 1.5g/kg body weight of a 20% glucose solution in PBS intraperitoneally. Blood was collected by tail bleeding at 0, 15, 30, 45, 90 and 120 minutes after injection of the glucose bolus to determine plasma glucose using either a portable glucometer or a glucose assay. In addition, body weight was determined.

Preparation of Stromal Vascular Fractions and CD11b$^+$ fraction

Dissected epididymal white adipose tissue (EWAT) was minced and Kreb's buffer (2.4M NaCl; 96 mMKCl; 24mM KH_2PO_4; 24mM $MgSO_4$ in Milli-Q; pH 7.4) was added. An equal volume of 2x collagenase I (Sigma) buffer was added and fat pads were incubated for 1h at 37°C in a shaking incubator at 60 rpm. The collagenase I was washed by adding prewarmed PBS and the suspension was strained through repeated pipetting and filtering through a 200uM filter. The suspension was washed and allowed to stand for 10 minutes to allow the fat cell to float. The infranatant was collected with a syringe and an 18G needle for SVF collection. SVF fraction was centrifuged for 10 minutes at 350G at RT. CD11b$^+$-cell isolation was performed through anti-CD11b antibody incubation conjugated to magnetic beads (Miltenyi Biotec). MACS columns were used to separate the stromal

vascular fraction (SVF) from the CD11b$^+$-cell -fraction following the manufacturer's protocol.

RNA Extraction and Real-time PCR

Total RNA from total Epididymal fat, SVF, and CD11b$^+$ fractions was obtrained through TRIzol (Invitrogen) extraction and the NucleoSpin II extraction kit (Macherey Nagel) according to manufacturer's protocol. cDNA was synthesized based on the measured RNA concentration (DeNovix DS-1) according to the manufacturer's protocol (Invitrogen). Real time qPCR was performed using Bio-Rad CFX96 Touch™ real-time PCR detection system (Bio-Rad Laboratories). Acidic ribosomal phosphoprotein 36B4 expression (*Rplp0*) was used as reference.

Plasma parameters

For plasma preparations, blood samples were collected via tail cut and collected in heparin coated capillaries at day 0 and 14 after 4 hours of fasting. Capillaries were centrifuged at 1500 rpm at 4°C. Plasma was collected and stored at -80°C until assayed. Plasma insulin levels were measured by ELISA (Crystal Chem Inc.) Whole blood was separately obtained at end of the treatment HbA1c was determined by using a Mouse Glycated Hemoglobin Assay Kit according to the manufacturers protocol (Crystal Chem Inc.).

Cell Culture Experiments

The macrophage cell line RAW264.7 (American Type Culture Collection, TIB-71) was cultured in DMEM supplemented with 10% fetal calf serum (Thermo Fisher Scientific), 1% glutamax (Thermo Fisher Scientific) and 0,2% antibiotics (penicillin-streptomycin) at 37°C at 5% CO_2 in a humidified chamber. In assays employing lysosomal perturbation, RAW264.7 cells were subjected to 80mM sucrose (Sigma) or 25mM HEPES (Sigma) for at least 24 hours. For siRNA mediated knock down experiments, RAW264.7 cells were seeded at a confluency of $3x10^5$ cells/ml and allowed to rest at least 3h before transfection. siRNA oligonucleotides were obtained from Qiagen and contained two sequences per target for Mitf (Sequence: SI02687692, SI0270963), Tfeb (Sequence: SI01444394, SI01444408) and Tfe3 (Sequence: SI01444415, SI05181435) and control (scrambled/SCR) siRNA (SI03650318). Cells were harvested 48 hours post-transfection and analysed on mRNA and protein expression.

Immunohistochemistry

EWAT was dehydrated in 70% ethanol overnight upon dissection, fixed in 4% formaline, phosphate-buffered at pH 7.0, and subsequently embedded in paraffin. Embedded tissue was cut in 4µm-thick sections, which were then deparaffinized by three 100% xylene washes and a subsequent 100% ethanol wash. Sections were rehydrated by washing subsequently in 96% ethanol, 70% ethanol and miliQ and heat induced epitope retrieval (HIER) was performed at 98°C for 10 minutes in 10mM citric acid (pH 6). Next, tissues were washed in PBS/0,1% Tween-20 (Sigma) and incubated with the following primary antibody rabbit-anti-Iba1 (Wako, 019-19741) diluted in PBS/5% antibody diluent (ScyTek Laboratories). Antibodies were visualized by Alexa Fluor™ 647 conjugated secondary anti rabbit antibody (Molecular Probes, A31573). For detection of transcription factors, cultured RAW264.7 on glass coverslips (VWR) were fixed in absolute methanol for 15

minutes at -20°C, blocked in 5% normal donkey serum (The Jackson Laboratory) diluted in 0.2% Tween/PBS. Cells were incubated with primary antibodies MITF (Exalpha BiologicalsInc, X1405M), TFEB (Bethyl Lab Inc, A303-673A) and TFE3 (Sigma, HPA023881) for 1h and detected with secondary anti mouse or rabbit Alexa Fluor™ 488 conjugated antibodies (Molecular Probes, A2102 and A21206 resp.).

Western Blot Analysis

Cultured RAW264.7 cells and tissue samples were lysed in radio immunoprecipitation assay (RIPA) buffer (150 mmol/L NaCl, 50 mmol/L Tris-HCl pH 7.4, 2 mmol/L EDTA, 0.5% deoxycholaat, 1 mmol/L Na_3VO_4, 20 mmol/L NaF, and 0.5% Triton X-100) containing protease and phosphatase inhibitors (Roche) and phenylmethylsulfonyl fluoride (PMSF; Sigma). Soluble lysate fraction was obtained by centrifugation at 12,000 x g for 15 minutes at 4°C. Protein concentrations were determined using the bicinchoninic acid assay (Thermo Fisher Scientific, 23225) and equal quantities of protein were denatured in Laemlli buffer at 95°C, separated on a 10% SDS-PAGE, and transferred to nitrocellulose (WELKE Biorad). Membranes were blocked in 5% (w:v) bovine serum albumin (Sigma, A1906) solution in PBS/0.1% Tween-20 (Sigma, P1379) for 1 h at room temperature (RT), and incubated overnight with respective antibodies at 4°C. Primary antibodies used MITF, TFEB and TFE3 (see earlier) and detected by using specific secondary conjugated antibodies (Alexa Fluor™ 488/647) (Molecular Probes). Detection of immunoblots was performed using a Typhoon FLA 9500 fluorescence scanner (GE Healthcare)

Statistical Analysis

Values presented in figures represent means ± standard deviation. Statistical analysis of expression data on the Gerp-siRNA treated groups was performed by Student *t* test (two tailed).

IPGTT analysis

With respect to IPGTT analysis, significance was established when $p \leq 0.05$ for a given difference in area under the curve (AUC) between groups, and the power of the effect is 80%, tested by a two-way ANOVA for repeated measurements.

References

1. Meijer, A. J. & Codogno, P. Autophagy: Regulation and role in disease autophagy, regulation, and disease A. J. Meijer and P. Codogno. *Crit. Rev. Clin. Lab. Sci.* **46,** 210–240 (2009).
2. Ballabio, A. & Bonifacino, J. S. Lysosomes as dynamic regulators of cell and organismal homeostasis. *Nat Rev. Mol. Cell. Biol.* **21,** 101–118 (2020).
3. Steingrímsson, E., Copeland, N. G. & Jenkins, N. A. Melanocytes and the *Microphthalmia* transcription factor network. *Annu. Rev. Genet.* **38**, 365–411 (2004).
4. Sardiello, M., Palmieri, M., Ronza, A. di, Medina, D. L., Valenza, M., *et al.* A gene network regulating lysosomal biogenesis and function. *Science* **325**, 473–477 (2009).
5. Pogenberg, V., Ögmundsdóttir, M. H., Bergsteinsdóttir, K., Schepsky, A., Phung, B., *et al.* Restricted leucine zipper dimerization and specificity of DNA recognition of the melanocyte master regulator MITF. *Genes Dev.* **26**, 2647–2658 (2012).
6. Moore, K. J. Insight into the microphthalmia gene. *Trends Genet.* **11**, 442–448 (1995).
7. Kim, D. H., Sarbassov, D. D., Ali, S. M., King, J. E., Latek, R. R., Erdjument-Bromage, H., Tempst, P. & Sabatini, D. M. mTOR interacts with raptor to form a nutrient-sensitive complex that signals to the cell growth machinery. *Cell* **110**, 163–175 (2002).
8. Düvel, K., Yecies, J. L., Menon, S., Raman, P., Lipovsky, A. I., Souza, A. L., Triantafellow, E., Ma, Q., Gorski, R., Cleaver, S., Vander Heiden, M. G., MacKeigan, J. P., Finan, P. M., Clish, C. B., Murphy, L. O. & Manning, B. D. Activation of a metabolic gene regulatory network downstream of mTOR Complex 1. *Mol. Cell* **39**, 171–183 (2010).
9. Zoncu, R., Bar-Peled, L., Efeyan, A., Wang, S., Sancak, Y. & Sabatini, D. M. mTORC1 senses lysosomal amino acids through an inside-out mechanism that requires the vacuolar H+-ATPase. *Science* **334**, 678–683 (2011).
10. Condon, K. J. & Sabatini, D. M. Nutrient regulation of mTORC1 at a glance. *J. Cell Sci.* **132**, (2019).
11. Sancak, Y., Peterson, T. R., Shaul, Y. D., Lindquist, R. A., Thoreen, C. C., Bar-Peled, L. & Sabatini, D. M. The rag GTPases bind raptor and mediate amino acid signaling to mTORC1. *Science* **320**, 1496–1501 (2008).
12. Jin, J., Smith, F. D., Stark, C., Wells, C. D., Fawcett, J. P., Kulkarni, S., Metalnikov, P., O'Donnell, P., Taylor, P., Taylor, L., Zougman, A., Woodgett, J. R., Langeberg, L. K., Scott, J. D. & Pawson, T. Proteomic, functional, and domain-based analysis of in vivo 14-3-3 binding proteins involved in cytoskeletal regulation and cellular organization. *Curr. Biol.* **14**, 1436–1450 (2004).
13. Roczniak-Ferguson, A., Petit, C. S., Froehlich, F., Qian, S., Ky, J., Angarola, B., Walther, T. C. & Ferguson, S. M. The transcription factor TFEB links mTORC1 signaling to transcriptional control of lysosome homeostasis. *Sci. Signal.* **5**, ra42 (2012).
14. Martina, J. A. & Puertollano, R. Rag GTPases mediate amino acid-dependent recruitment of TFEB and MITF to lysosomes. *J. Cell Biol.* **200**, 475–491 (2013).
15. Martina, J. A., Diab, H. I., Brady, O. A. & Puertollano, R. TFEB and TFE3 are novel components of the integrated stress response. *EMBO J.* **35**, 479–495 (2016).
16. Martina, J. A., Chen, Y., Gucek, M. & Puertollano, R. MTORC1 functions as a transcriptional regulator of autophagy by preventing nuclear transport of TFEB. *Autophagy* **8**, 903–914 (2012).
17. Bronisz, A., Sharma, S. M., Hu, R., Godlewski, J., Tzivion, G., Mansky, K. C. & Ostrowski, M. C. Microphthalmia-associated transcription factor interactions with 14-3-3 modulate differentiation of committed myeloid precursors. *Mol. Biol. Cell* **17**, 3897–3906 (2006).
18. Settembre, C., Di Malta, C., Polito, V. A., Arencibia, M. G., Vetrini, F., Erdin, S., Erdin, S. U., Huynh, T., Medina, D., Colella, P., Sardiello, M., Rubinsztein, D. C. & Ballabio, A. TFEB links autophagy to lysosomal biogenesis. *Science* **332**, 1429–1433 (2011).

19. Settembre, C., Zoncu, R., Medina, D. L., Vetrini, F., Erdin, S. S. S., Erdin, S. S. S., Huynh, T., Ferron, M., Karsenty, G., Vellard, M. C., Facchinetti, V., Sabatini, D. M. & Ballabio, A. A lysosome-to-nucleus signalling mechanism senses and regulates the lysosome via mTOR and TFEB. *EMBO J.* **31**, 1095–1108 (2012).

20. Spampanato, C., Feeney, E., Li, L., Cardone, M., Lim, J.-A., Annunziata, F., Zare, H., Polishchuk, R., Puertollano, R., Parenti, G., Ballabio, A. & Raben, N. Transcription factor EB (TFEB) is a new therapeutic target for Pompe disease. *EMBO Mol. Med.* **5**, 691–706 (2013).

21. Song, W., Wang, F., Savini, M., Ake, A., di Ronza, A., Sardiello, M. & Segatori, L. TFEB regulates lysosomal proteostasis. *Hum. Mol. Genet.* **22**, 1994–2009 (2013).

22. Medina, D. L., Fraldi, A., Bouche, V., Annunziata, F., Mansueto, G., Spampanato, C., Puri, C., Pignata, A., Martina, J. A., Sardiello, M., Palmieri, M., Polishchuk, R., Puertollano, R. & Ballabio, A. Transcriptional activation of lysosomal exocytosis promotes cellular clearance. *Dev. Cell* **21**, 421–30 (2011).

23. Folick, A., Oakley, H. D., Yu, Y., Armstrong, E. H., Kumari, M., Sanor, L., Moore, D. D., Ortlund, E. A., Zechner, R. & Wang, M. C. Lysosomal signaling molecules regulate longevity in Caenorhabditis elegans. *Science* **347**, 83–86 (2015).

24. Peng, W., Minakaki, G., Nguyen, M. & Krainc, D. Preserving lysosomal function in the aging brain: insights from neurodegeneration. *Neurotherapeutics* **16**, 611–634 (2019).

25. Perera, R. M., Stoykova, S., Nicolay, B. N., Ross, K. N., Fitamant, J., Boukhali, M., Lengrand, J., Deshpande, V., Selig, M. K., Ferrone, C. R., Settleman, J., Stephanopoulos, G., Dyson, N. J., Zoncu, R., Ramaswamy, S., Haas, W. & Bardeesy, N. Transcriptional control of autophagy–lysosome function drives pancreatic cancer metabolism. *Nature* **524**, 361–365 (2015).

26. Kimmelman, A. C. & White, E. Autophagy and tumor metabolism. *Cell Metabolism* **25**, 1037–1043 (2017).

27. Jaishy, B. & Abel, E. D. Lipotoxicity: Many roads to cell dysfunction and cell death lipids, lysosomes, and autophagy. *J. Lipid Res.* **57**, 1619–1635 (2016).

28. Gilleron, J., Gerdes, J. M. & Zeigerer, A. Metabolic regulation through the endosomal system. *Traffic* **20**, 552–570 (2019).

29. Xu, X., Grijalva, A., Skowronski, A., van Eijk, M., Serlie, M. J. J., Ferrante, A. W. W., van Eijk, M., Serlie, M. J. J. & Ferrante, A. W. W. Obesity activates a program of lysosomal-dependent lipid metabolism in adipose tissue macrophages independently of classic activation. *Cell Metab.* **18**, 816–830 (2013).

30. Gabriel, T. L., Tol, M. J., Ottenhof, R., van Roomen, C., Aten, J., *et al.* Lysosomal stress in obese adipose tissue macrophages contributes to MITF-dependent Gpnmb induction. *Diabetes* **63**, 3310–3323 (2014).

31. Van Der Lienden, M. J. C., Gaspar, P., Boot, R., Aerts, J. M. F. G. & Van Eijk, M. Glycoprotein non-metastatic protein B: An emerging biomarker for lysosomal dysfunction in macrophages. *Int. J. Mol. Sci.* **20** 66 (2019).

32. Wang, Z. V & Scherer, P. E. Adiponectin, the past two decades. *J. Mol. Cell Biol.* **8** 93–100 (2016).

33. Aouadi, M., Tencerova, M., Vangala, P., Yawe, J. C., Nicoloro, S. M., Amano, S. U., Cohen, J. L. & Czech, M. P. Gene silencing in adipose tissue macrophages regulates whole-body metabolism in obese mice. *Proc. Natl. Acad. Sci. USA.* **110**, 8278–8283 (2013).

34. Aouadi, M., Vangala, P., Yawe, J. C., Tencerova, M., Nicoloro, S. M., Cohen, J. L., Shen, Y. & Czech, M. P. Lipid storage by adipose tissue macrophages regulates systemic glucose tolerance. *Am. J. Physiol. - Endocrinol. Metab.* **307**, (2014).

35. Hill, D. A., Lim, H. W., Kim, Y. H., Ho, W. Y., Foong, Y. H., Nelson, V. L., Nguyen, H. C. B., Chegireddy, K., Kim, J., Habertheuer, A., Vallabhajosyula, P., Kambayashi, T., Won, K. J. & Lazar, M. A. Distinct macrophage populations direct inflammatory versus physiological

changes in adipose tissue. *Proc. Natl. Acad. Sci. USA.* **115**, E5096–E5105 (2018).

36. Jaitin, D. A., Adlung, L., Thaiss, C. A., Weiner, A., Li, B., *et al.* Lipid-associated macrophages control metabolic homeostasis in a Trem2-dependent manner. *Cell* **178**, 686-698.e14 (2019).

37. Yasumoto, K. I., Amae, S., Udono, T., Fuse, N., Takeda, K. & Shibahara, S. A big gene linked to small eyes encodes multiple Mitf isoforms: many promoters make light work. *Pigment Cell Res.* **11** 329–336 (1998).

38. Louphrasitthiphol, P., Siddaway, R., Loffreda, A., Pogenberg, V., Friedrichsen, H., *et al.* Tuning transcription factor availability through acetylation-mediated genomic redistribution. *Mol. Cell* (2020)

39. Martínez-Fábregas, J., Prescott, A., van Kasteren, S., Pedrioli, D. L., McLean, I., Moles, A., Reinheckel, T., Poli, V. & Watts, C. Lysosomal protease deficiency or substrate overload induces an oxidative-stress mediated STAT3-dependent pathway of lysosomal homeostasis. *Nat. Commun.* **9**, 1–16 (2018).

40. Chauhan, S., Goodwin, J. G., Chauhan, S., Manyam, G., Wang, J., Kamat, A. M. & Boyd, D. D. ZKSCAN3 Is a Master Transcriptional Repressor of Autophagy. *Mol. Cell* **50**, 16–28 (2013).

41. Li, Y., Xu, M., Ding, X., Yan, C., Song, Z., *et al.* Protein kinase C controls lysosome biogenesis independently of mTORC1. *Nat. Cell Biol.* **18**, 1065–1077 (2016).

42. Annunziata, I., van de Vlekkert, D., Wolf, E., Finkelstein, D., Neale, G., Machado, E., Mosca, R., Campos, Y., Tillman, H., Roussel, M. F., Andrew Weesner, J., Ellen Fremuth, L., Qiu, X., Han, M. J., Grosveld, G. C. & D'Azzo, A. MYC competes with MiT/TFE in regulating lysosomal biogenesis and autophagy through an epigenetic rheostat. *Nat. Commun.* **10**, 3623 (2019).

43. Pastore, N., Brady, O. A., Diab, H. I., Martina, J. A., Sun, L., Huynh, T., Lim, J.-A., Zare, H., Raben, N., Ballabio, A. & Puertollano, R. TFEB and TFE3 cooperate in the regulation of the innate immune response in activated macrophages. *Autophagy* **12**, 1240–1258 (2016).

44. Prieur, X., Mok, C. Y. L., Velagapudi, V. R., Núñez, V., Fuentes, L., Montaner, D., Ishikawa, K., Camacho, A., Barbarroja, N., O'Rahilly, S., Sethi, J. K., Dopazo, J., Orešič, M., Ricote, M. & Vidal-Puig, A. Differential lipid partitioning between adipocytes and tissue macrophages modulates macrophage lipotoxicity and M2/M1 polarization in obese mice. *Diabetes* **60**, 797–809 (2011).

45. Kratz, M., Coats, B. R., Hisert, K. B., Hagman, D., Mutskov, V., Peris, E., Schoenfelt, K. Q., Kuzma, J. N., Larson, I., Billing, P. S., Landerholm, R. W., Crouthamel, M., Gozal, D., Hwang, S., Singh, P. K. & Becker, L. Metabolic dysfunction drives a mechanistically distinct proinflammatory phenotype in adipose tissue macrophages. *Cell Metab.* **20**, 614–625 (2014).

46. Coats, B. R., Schoenfelt, K. Q., Barbosa-Lorenzi, V. C., Peris, E., Cui, C., Hoffman, A., Zhou, G., Fernandez, S., Zhai, L., Hall, B. A., Haka, A. S., Shah, A. M., Reardon, C. A., Brady, M. J., Rhodes, C. J., Maxfield, F. R. & Becker, L. Metabolically activated adipose tissue macrophages perform detrimental and beneficial functions during diet-induced obesity. *Cell Rep.* **20**, 3149–3161 (2017).

47. Russo, L. & Lumeng, C. N. Properties and functions of adipose tissue macrophages in obesity. *Immunology* **155**, 407–417 (2018).

48. Lee, Y. S., Wollam, J. & Olefsky, J. M. An integrated view of immunometabolism. *Cell* **172**, 22–40 (2018).

49. Stern, J. H., Rutkowski, J. M. & Scherer, P. E. Adiponectin, leptin, and fatty acids in the maintenance of metabolic homeostasis through adipose tissue crosstalk. *Cell Metab.* **23** 770–784 (2016).

50. Tesz, G. J., Aouadi, M., Prot, M., Nicoloro, S. M., Boutet, E., Amano, S. U., Goller, A., Wang, M., Guo, C.-A., Salomon, W. E., Virbasius, J. V, Baum, R. A., O'Connor, M. J., Soto, E.,

Ostroff, G. R. & Czech, M. P. Glucan particles for selective delivery of siRNA to phagocytic cells in mice. *Biochem. J.* **436**, 351–62 (2011).

Supplemental Figures

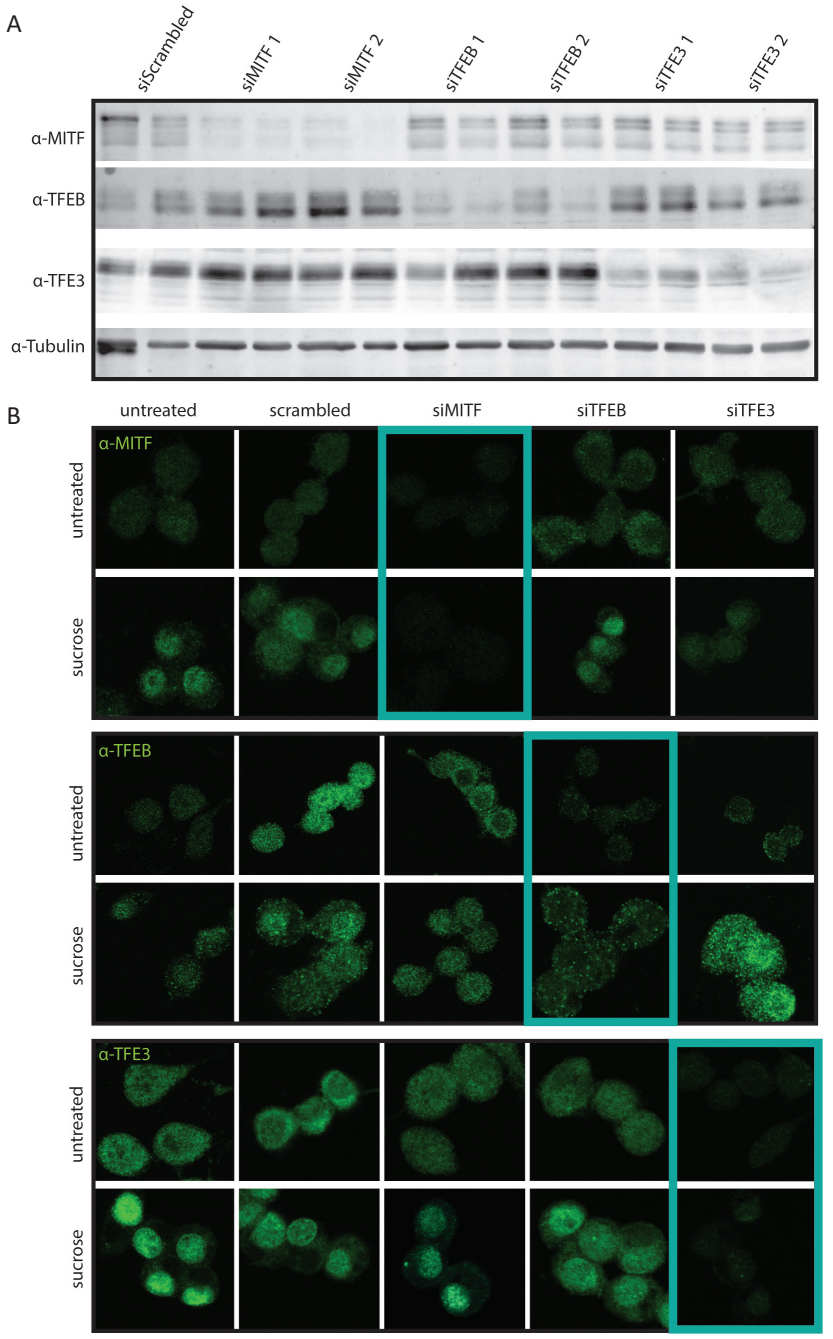

Supplemental figure 1. Validation of siRNA mediated knock down of Mitf, Tfeb and Tfe3 on protein level; *(**A**) Verification of specificity target genes by two oligonucleotide sequences per gene. (**B**) Immunocytochemical validation of subcellular localization and intensity MiT/TFE members upon single knock down of either Mitf, Tfeb or Tfe3.*

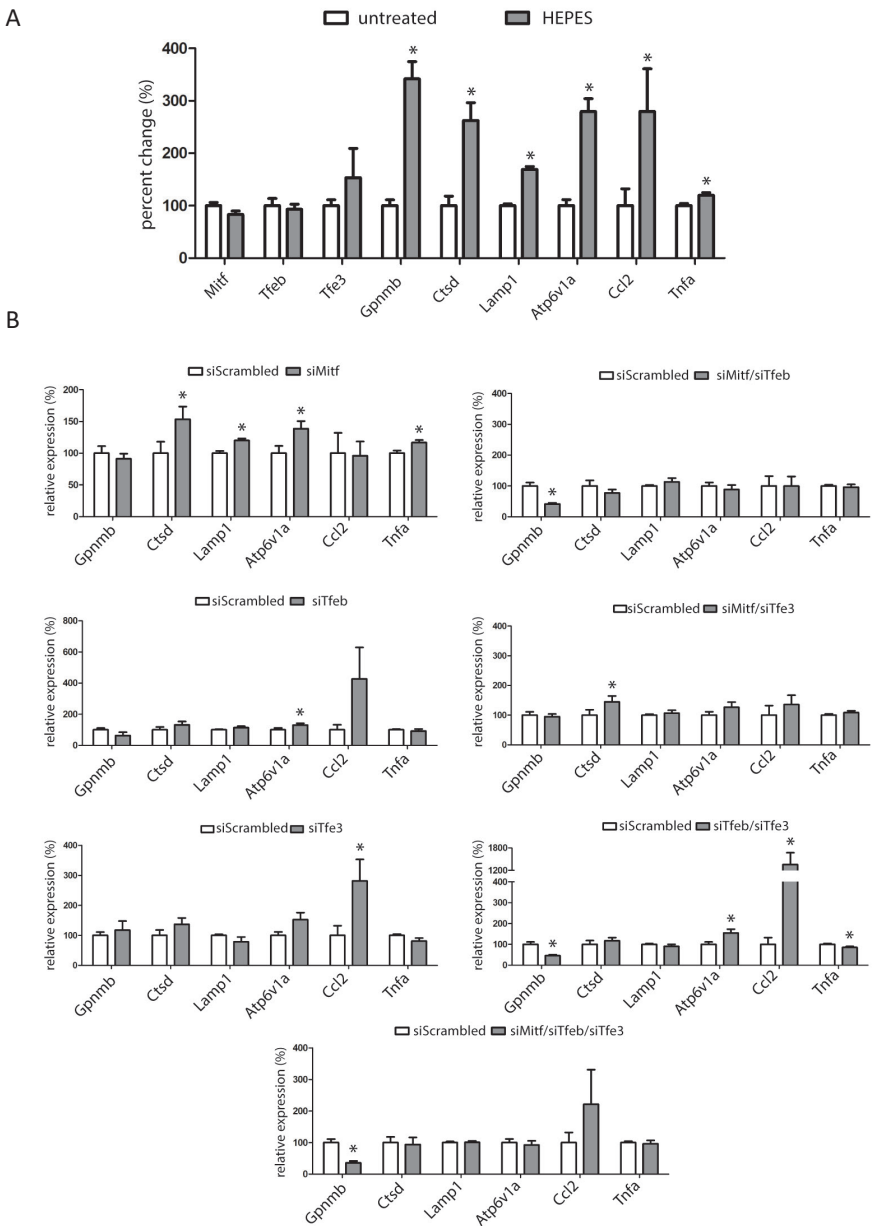

Supplemental figure 2. Gene expression analysis of lysosome related genes *upon* ***(A)*** *HEPES addition to medium,* ***(B)*** *combinatorial knock down of Mitf, Tfeb and Tfe3 under (non-stressed) basal conditions;* ***(C; Next page ->)*** *inflammatory gene expression analysis during combinatorial knock down of Mitf, Tfeb and Tfe3 and (non-stressed) basal conditions*

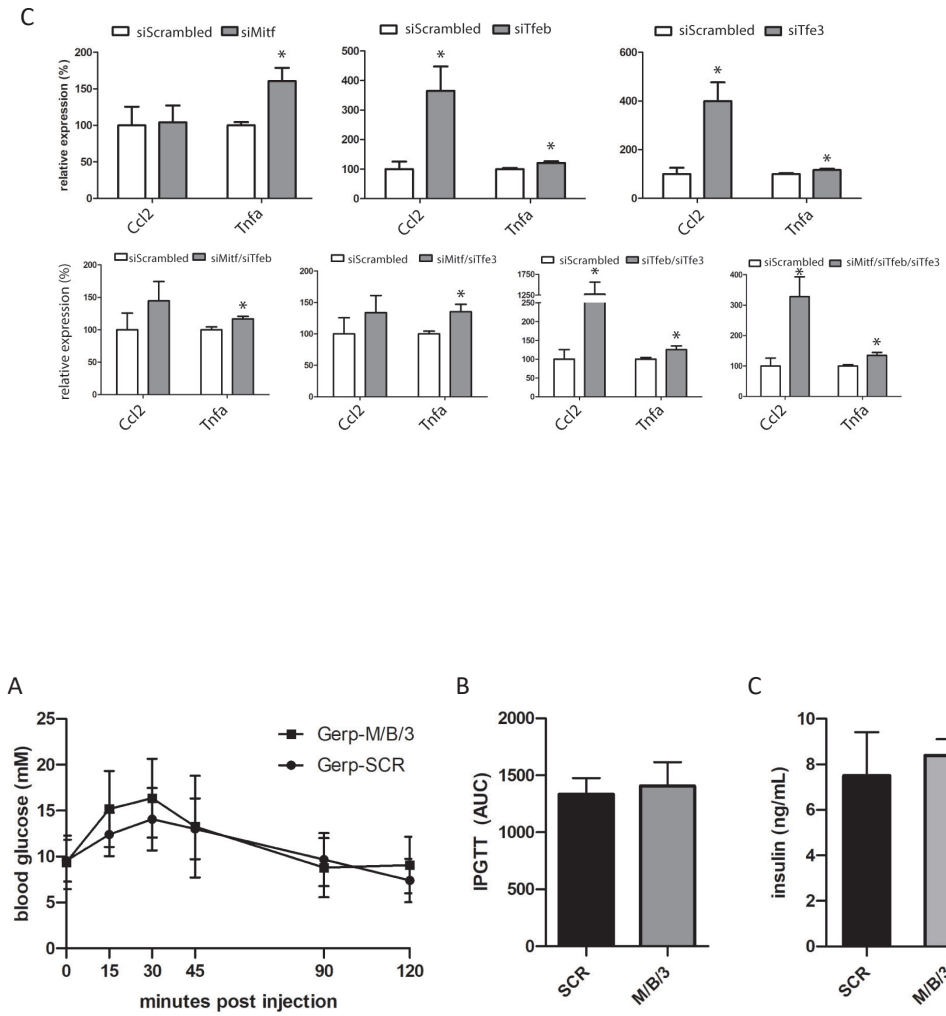

***Supplemental figure 3. Metabolic parameters of mice at start of experiment**; (**A**) Time curve of Intraperitoneal glucose tolerance test (IPGTT) of scrabled siRNA-Gerp and siMiT/TFE-Gerp treated group; (**B**) Area under the curve (AUC) of IPGTT; (**C**) Blood insulin levels*